16th World Conference on Earthquake Engineering, 16WCEE 2017

Santiago Chile, January 9th to 13th 2017

Paper N° 2593

Registration Code: S-W1463099704

ANALYSIS OF SHEAR-DOMINATED RC COLUMNS USING THE NONLINEAR TRUSS ANALOGY

M. Moharrami[1], I. Koutromanos[2], M. Panagiotou[3], and S.C. Girgin[4]

[1] *Graduate Student, Department of Civil and Environmental Engineering, Virginia Polytechnic Institute and State University, Blacksburg, VA, mrmg@vt.edu.*

[2] *Assistant Professor, Department of Civil and Environmental Engineering, Virginia Polytechnic Institute and State University, Blacksburg, VA, ikoutroum@vt.edu.*

[3] *Senior Consultant, Nabih Youssef Structural Engineers, Los Angeles, CA, mpanagiotou@nyase.com.*

[4] *Research Assistant, Department of Civil Engineering, Dokuz Eylul University, Izmir, Turkey, scgirgin@gmail.com.*

Abstract

This study uses the nonlinear truss analogy for the simulation of shear failures in reinforced concrete (RC) columns. A previously established method, aimed to the analysis of RC walls, is enhanced to allow simulations of column members. The concrete constitutive equations are modified to account for the contribution of the aggregate interlock to the shear resistance. Additionally, an equation is proposed to determine the inclination angle of the diagonal members in the truss models. The modeling approach is validated through nonlinear analysis of RC columns and frames subjected to quasi-static and dynamic loads. The combination of predictive capabilities and conceptual simplicity establishes truss-based models as an attractive approach for the systematic analysis of shear-dominated, RC frame construction.

Keywords: reinforced concrete; nonlinear truss model; shear-dominated columns; seismic loading; aggregate interlock.

1. Introduction

Reinforced concrete frame (RCF) structures represent a significant portion of the building inventory in the United States [1]. The design of older construction of this type has been dominated by gravity load considerations, without appropriate detailing to prevent the occurrence of shear failures under strong earthquakes [2,3]. Furthermore, many RCF buildings in the less seismically active Central and Eastern United States are designed as ordinary moment frames according to ACI 318-11 [4]. These types of frames have not been detailed with capacity design principles which ensure that the occurrence of flexure-dominated inelastic modes precedes that of the less ductile, shear-dominated modes. Since shear-induced failures are possible for both old and several modern RCF buildings when subjected to lateral loads, the reliable determination of the seismic response of such structures critically hinges on the capability to simulate the effect of column shear damage on the structural response.

The simplest modeling method for the analysis of shear failures in RCF columns is based on combinations of beam-based models and nonlinear springs to capture the strength and stiffness degradation associated with shear damage and also the shear-flexure interaction [5,6,7]. Such springs typically rely on empirical equations which provide estimates of the lateral deformations at which shear failure will occur [8]. The model by Elwood [5] was used by Elwood and Moehle [6] to capture the response of a three-column, shake-table RCF specimen for which the middle column incurred shear failure. The analysis provided satisfactory estimates of the response of the specimen until the occurrence of shear failure, after which point the lateral displacements of the structure were underestimated. Leborgne and Ghannoum [7] have shown that their model can capture the results of various quasi-static experimental tests on shear-dominated columns; despite the establishment of algorithms to calibrate the model from experimental data, manual adjustments may still be required to achieve the best possible agreement with experimental results [9]. Additionally, the physical meaning of several parameters in the model, affecting the hysteretic behavior and strength degradation with repeated loading, is somewhat obscure, since it cannot be directly related to the mechanical behavior. The same applies for the model formulated by Elwood [5]. Expressions have also been proposed to capture the effect of shear damage on the occurrence of column axial failure [10], defined as the inability of a column to carry its gravity loads due to the shear damage and pertinent geometric nonlinearity effects.

A number of alternative modeling approaches, formulated at the material ("stress-strain") level, can be used to analyze shear-dominated RC members. The most refined method of this kind is based on the use of nonlinear finite element models, which have been employed in several analyses of shear damage in reinforced concrete (RC) columns with satisfactory results [11,12]. Finite element models are computationally demanding and commonly require many material parameters to be calibrated. Additionally, advanced formulations like non-local constitutive models or cohesive crack interface elements (e.g., [12]) are usually needed to capture the effect of large inclined cracks on the response.

Several studies have used nonlinear truss models for capturing the response of two-dimensional [13,14,15] and three-dimensional [16,17] RC components, with very satisfactory results. Truss models are conceptually simpler than finite element models, since they essentially rely on relatively simple, uniaxial material laws. Unlike nonlinear spring models, the calibration of truss models is straightforward and can rely on material test data. Satisfactory results have been reported for slender, flexure-dominated RC beams [14] and for RC walls [15,17]; however, the accuracy of the method for the analysis of shear-dominated RC columns remains to be demonstrated.

Nonlinear truss models are used in this paper to capture the shear-induced failure of RC columns under cyclic loading. A recently established methodology [15,17], developed for the analysis of shear walls, is enhanced to allow the simulation of column structures. A simple equation is proposed to determine the angle of the diagonal elements of a nonlinear truss model. Furthermore, the concrete material laws are modified to account for the effect of aggregate interlock across an inclined shear crack. The proposed analysis method is validated using the results of two quasi-static and one shake-table test on shear-dominated RC columns. Additional analyses are conducted to demonstrate the effect of the aggregate interlock and of the inclination angle of the diagonal elements on the analytical results.

2. Description of Analysis Methodology

The nonlinear truss model represents a RC column as an assemblage of horizontal, vertical and diagonal truss elements, as shown in Fig. 1.

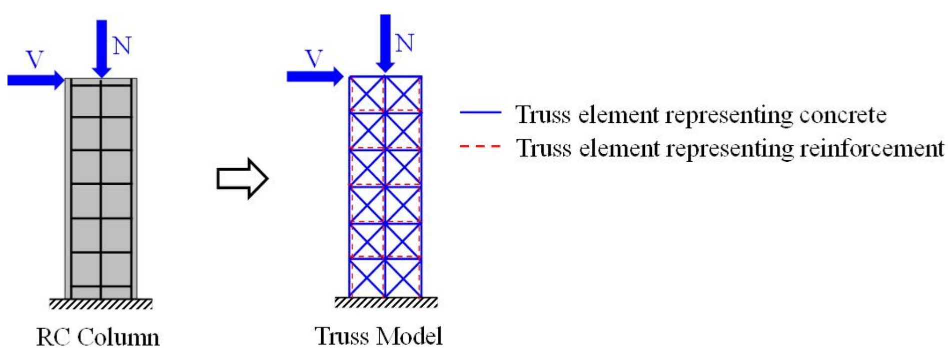

Fig. 1 – Truss modeling of cantilever RC column.

2.1. Determination of truss geometry

This section provides guidelines to establish the geometry of a truss representation of a RC column. More specifically, the procedure to obtain the cross-sectional area of the various truss elements and the inclination angle of the diagonal members is presented.

2.1.1. Vertical elements

The first step for the establishment of a truss model is the determination of the location and of the cross-sectional properties of the vertical elements. The outermost vertical elements are placed at the location of the centroid of the outermost vertical steel reinforcement. The tributary sectional depths of the various vertical elements are then determined by equally subdividing the region between neighboring elements. The cross-sectional area of each concrete vertical element is the product of the tributary depth and *t*, with *t* being the out-of-plane width of the cross-section of the column.

2.1.2. Diagonal elements

The inclination angle of the diagonal elements of a truss model is established based on the assumption that the direction of the diagonal compressive field is parallel to the initial crack that occurs under the combined effect of compressive axial force and shear force. While this assumption is not perfectly accurate, it leads to a conceptually simple procedure for the establishment of the inclination angle [18].The stress state is characterized by the uniform compressive stress, σ and the uniform stress due to shear force, τ, acting on a horizontal (sectional) plane. In this case, the direction angle, θ_p, of the maximum principal stress, i.e. the angle between maximum principal stress and horizontal axis, is given by:

$$\tan\left(2\theta_p\right) = \frac{2\tau}{-\sigma} \tag{1}$$

Since, the direction of the diagonal crack is assumed to be perpendicular to the principal stress, the inclination angle θ_d of the diagonal crack and the diagonal members is given by:

$$\theta_d = 90^o - \theta_p \tag{2}$$

Once the inclination angle of the diagonal elements has been established, their sectional depth, b_d, can be determined, as shown in Fig. 2a, in accordance with the following equation [15]:

$$b_d = b \cdot \sin\theta_d \tag{3}$$

where b is the spacing of the vertical elements in the truss model. The use of Eq. (3) for the determination of b_d has been shown to provide good estimates of the strength and stiffness contributed by the diagonal members of the truss model.

2.1.3. Horizontal Elements

After the location of the vertical elements and the inclination angle of the diagonal elements have been determined, the truss geometry is finalized by establishing the location and cross-sectional area of the horizontal elements. The cross-sectional depth of the horizontal elements is obtained by equally dividing the height between consecutive horizontal elements. The obtained sectional depth is multiplied by t to give the cross-sectional area of each horizontal truss element. If the amount and spacing of the transverse reinforcement are constant over a column segment, the cross-sectional area of the truss elements representing the horizontal steel reinforcement in that segment is obtained by dividing the total amount of transverse reinforcement in the segment by the corresponding number of horizontal truss elements. An example determination of the cross-sectional areas of the five horizontal elements of the truss model for a column segment is presented in Fig. 2b.

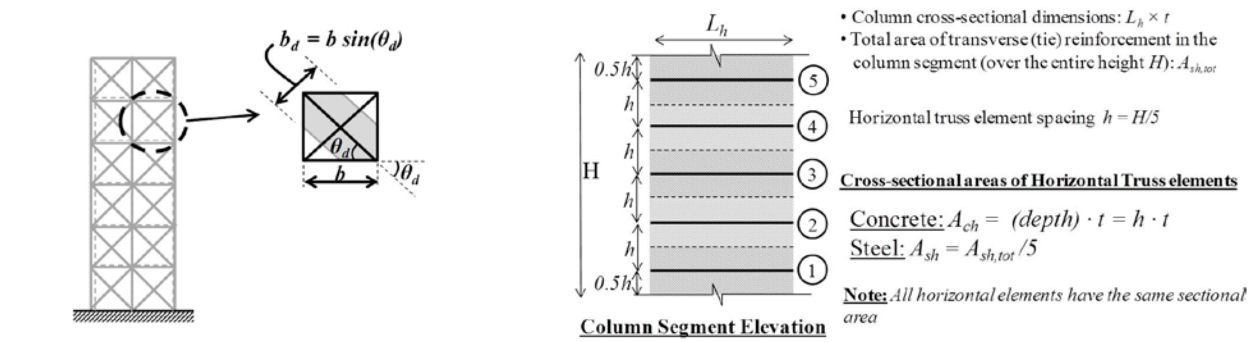

(a) Sectional depth of diagonal elements (b) Determination of sectional areas for horizontal elements

Fig. 2 – Determination of geometry for diagonal and horizontal truss elements

2.2. Constitutive laws

The truss modeling approach uses a set of uniaxial constitutive laws to capture the salient features affecting the hysteretic behavior of columns. This section describes the material models employed herein.

2.2.1. *Concrete*

The uniaxial material model for concrete is the one developed and used in [17]. As shown in Fig. 3a, the concrete constitutive law can capture the strength and stiffness degradation due to inelastic compressive and tensile strains. Softening in the tensile regime can be described by either an exponential or a trilinear curve. If properly calibrated, the material model can also capture the behavior of confined concrete, as shown in Fig. 3a. The concrete constitutive law of the diagonal truss members accounts for the instantaneous effect of transverse tensile strains on the compressive resistance, in accordance with experimental observations by Vecchio and Collins [19]. To this end, at every step in an analysis, the diagonal compressive stresses are multiplied by a reduction coefficient, β, which expresses the adverse effect of transverse tension on the compressive stress of concrete. Thus, every diagonal truss element requires the definition of an additional pair of nodes to establish a fictitious "strain gauge" element which allows the calculation of the transverse strain, as shown in Fig. 3b and explained in detail in [15,17].

The constitutive model for concrete involves softening, and thus the stress-strain laws must be regularized to prevent the spurious dependence of the analysis results on the size of the mesh, as explained, e.g., in [20]. The parameters pertaining to compressive inelastic strains are regularized according to [17]. Panagiotou et al. [15] have shown that the equation giving the variation of the reduction coefficient β with the transverse tensile strain must also be adjusted with element size. The regularization procedure described in [17] is used for the calibration of the constitutive equations giving the variation of β with transverse strain.

2.2.2. Reinforcing steel

The truss elements representing the longitudinal and transverse reinforcement use the Giuffre-Menegotto-Pinto (GMP) material model [21]. The specific material model is characterized by a monotonic envelope curve with linear hardening after yielding. Additionally, the model can account for the nonlinear hysteretic behavior of reinforcing steel, as shown in Fig. 3c. A detailed explanation of the GMP model, including the mathematical expressions which describe the nonlinear unloading-reloading curves, is provided in [21]. The GMP model cannot capture the effects of bar buckling and rupture on the stress-strain response of the reinforcing steel. Such effects exist in flexure-dominated members where the longitudinal reinforcement is subjected to large inelastic deformations and they are not expected to be significant for the shear-dominated columns considered here.

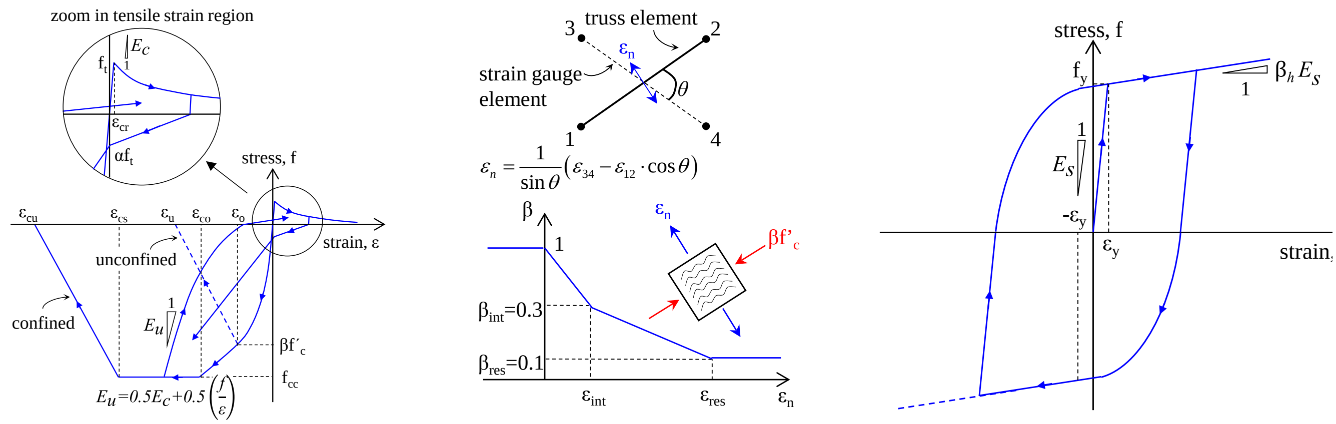

(a) Stress-strain law for concrete (b) Calculation of transverse strain (c) Stress-strain law for steel

Fig. 3 – Constitutive models for concrete and reinforcing steel.

2.2.3. Accounting for aggregate interlock effect in cracked concrete

The proposed modeling approach can also capture the effect of aggregate interlock on the resistance of inclined concrete cracks. This effect must be accounted for in slender RC members like columns, as discussed in [18] and schematically explained in Fig. 4. The figure presents the shear force transfer between two consecutive compressive diagonals (1-2-3) and (4-5-6) of a truss model representing a RC column. The concrete material of the horizontal and diagonal elements under tension is assumed to have completely lost its tensile strength. It can be verified from Fig. 4a that horizontal (shear) force transfer from (1-2-3) to (4-5-6) can only occur through tension in the horizontal steel of elements (4-2) and (5-3). It becomes obvious that the shear force in the column cannot exceed the value V_s corresponding to the contribution of the column transverse reinforcement to the shear resistance.

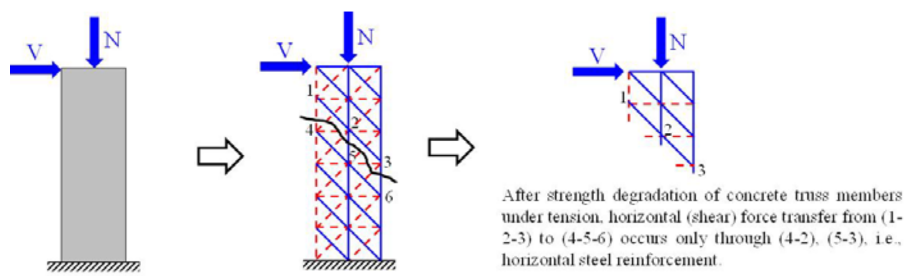

Fig. 4 – Force transfer after tensile cracking and loss of tensile strength of the diagonals in truss model of a slender column

Based on the above, if a truss model is used for the analysis of slender members such as RC columns, the material laws of the horizontal elements need to somehow account for the contribution V_c of the concrete to the shear resistance. The aggregate interlock is accounted for through the combination of several simplifying assumptions and a previously proposed equation [22] for the estimation of the shear resistance across a crack. The basic assumption made is that the cracks form at an angle equal to that of the diagonal members, θ_d. Additionally, the overall crack displacement vector is assumed to be parallel to the horizontal direction. If the crack displacement magnitude, $u_{cr,h}$, is known, then the crack-normal displacement, w, and the crack-parallel displacement, s, can be obtained from the following expressions, in accordance with Fig. 5a:

$$w = u_{cr,h} \cdot \sin\theta_d \tag{4a}$$

$$s = u_{cr,h} \cdot \cos\theta_d \tag{4b}$$

Once *w* and *s* are obtained, the shear stress along the inclined crack plane can be calculated using the following equation [22].

$$\tau = -\frac{f_{cc}}{30} + \left[1.80w^{-0.8} + \left(0.234w^{-0.71} - 0.20\right)f_{cc}\right]s \tag{5}$$

where f_{cc} is the compressive cube strength of the material (in MPa), which can be conservatively set equal to the cylinder compressive strength, f_c. The displacement components w and s in Eq. (5) must be expressed in mm.

The inclined resultant force due to the aggregate interlock is equal to the product of τ and the corresponding area of the inclined crack plane, $L_d \times t$, as shown in Fig. 5b. The horizontal component of this force is:

$$F_{a,h} = \tau \cdot L_d \cdot \cos\theta_d \cdot t \tag{6}$$

where L_d is the length of the inclined crack plane. In the truss models used here, the force $F_{a,h}$ due to aggregate interlock is carried by the horizontal members. The additional stress that each horizontal member needs to carry is obtained by dividing the force $F_{a,h}$ by the corresponding cross-sectional area of concrete.

$$\sigma_{a,h} = \frac{F_{a,h}}{h \times t} = \frac{\tau \cdot L_d \cdot \cos\theta_d \cdot t}{h \cdot t} = \frac{\tau \cdot h / \sin\theta_d \cdot \cos\theta_d \cdot t}{h \cdot t} = \frac{\tau \cdot \cos\theta_d}{\sin\theta_d} = \frac{\tau}{\tan\theta_d} \tag{7}$$

where h is the vertical distance between horizontal truss elements.

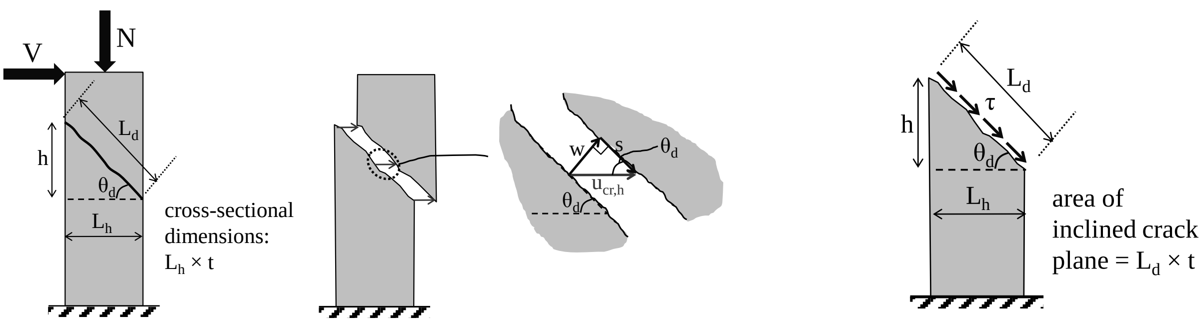

(a) Crack geometry and displacement discontinuity (b) shear stresses along crack plane

Fig. 5 – Aggregate interlock model

2.2.4. Accounting for Strain Penetration Effects

The models presented herein account for the strain penetration effect at locations where flexural inelasticity is expected to occur for column members. This is accomplished by introducing additional vertical elements with length equal to L_b [23]. Given the value s_y, of the total slip at yield, L_b can be obtained by stipulating that the uplift due to the additional vertical elements – which, at the onset of yield of the vertical reinforcement, will have an axial strain equal to ε_y – is equal to s_y:

$$s_y = \varepsilon_y \cdot L_b \rightarrow L_b = s_y / \varepsilon_y \tag{13}$$

3. Verification of Analysis Methodology

The modeling approach based on the truss analogy has been validated with the results of quasi-static and dynamic tests on RC column specimens. The analyses have been conducted using the nonlinear analysis program OpenSees [24] which includes the element formulations and constitutive laws of the methodology described in Section 2. The parameters of the analytical models are presented in Tables 1, 2 and 3. Table 1 presents the cross-sectional areas of the various elements in the truss models, and Tables 2 and 3 present concrete and steel material properties, respectively.

Table 1 – Cross-sectional areas for Truss elements

Specimen	A_{svb} (mm^2)	A_{svw} (mm^2)	A_{sh} (mm^2)	A_{cvb} (mm^2)	A_{cvw} (mm^2)	A_{ch} (mm^2)	A_{cd} (mm^2)
Priestley et al. R1A	1425	1140	100	42833	53998	76202	44058
Priestley et al. R3A	1425	1140	93	42833	53998	70759	42926
Elwood and Moehle	451	395	57	17013	18874	26061	15286

Note : A_{svb} = Area of outermost vertical steel elements, A_{svw} = Area of interior vertical steel elements, A_{sh} = Area of horizontal steel elements, A_{cvb} = Area of outermost vertical concrete elements, A_{svw} = Area of interior vertical concrete elements, A_{ch} = Area of horizontal concrete elements, A_{cd} = Area of diagonal elements

3.1. Quasi-static tests

The first set of verification analyses is conducted for two shear-dominated columns tested by Priestley et al. [25].The configuration and cross-sectional reinforcement for the two specimens, termed R1A and R3A, are shown in Fig. 6. The same figure presents the geometry of the truss models. Both specimens were restrained against rotation at both ends and were subjected to a cyclic displacement history at the top. The axial load was equal to 510 kN (114 kip) for both specimens, while the concrete compressive strength was equal to 37.8 MPa (5.5 ksi) for specimen R1A and 34.4 MPa (5.0 ksi) for specimen R3A. The longitudinal reinforcement consisted of 19 mm - diameter (No. 6) deformed bars, and the transverse reinforcement was 6 mm – diameter (No. 2) ties with a spacing of 127 mm (5 in.). The longitudinal and transverse reinforcement ratios were equal to 0.0254 and 0.0012, respectively, for both specimens. The main difference between the two specimens was that the yield stress of the longitudinal reinforcement was equal to 323 MPa (47 ksi) for specimen R1A and 467 MPa (68 ksi) for specimen R3A, and the yield stress of the transverse reinforcement was equal to 357 MPa (52 ksi) for specimen R1A and 323 MPa (47 ksi) for specimen R3A. The two specimens incurred strength degradation due to shear damage at drift ratios of 1.40% and 0.95%, respectively.

The analytically obtained hysteretic response for the two specimens is compared to the corresponding experimental observations in Figs. 7a and 7b, for columns R1A and R3A, respectively. It can be seen that the truss models provide very good estimates of the load-displacement response of the two specimens, including the significant strength degradation obtained due to shear damage. As shown in Figs. 8a and 8b, the strength degradation in the analyses was caused by the occurrence of inclined cracks, just like in the experimental tests.

Table 2 – Material Parameters for Concrete

Specimen	f'_c (MPa)	E_c (MPa)	f_t (MPa)	Vertical Elements				Horizontal Elements			
				ε_{cres}	ε_{cint}	f_{cint} (MPa)	M	ε_{tres}	f_{tres} (MPa)	ε_{tint}	f_{tint} (MPa)
Priestley et. al R1A	-38	38000	2.03	-0.0113	-0.0066	19.00	0.131, 0.083	0.012	0.031	0.0025	1.8
Priestley et. al R3A	-34	34000	3.40	-0.0121	-0.0071	17.00	0.131, 0.083	0.012	0.052	0.0026	1.7
Elwood & Moehle	-24.5	24500	2.45	-0.0183	-0.010	12.25	0.144, 0124	0.022	0.001	0.0017	1.1

Note 1: ε_{cres} = strain at which the concrete completely loses compressive strength, M = parameter affecting the tensile strength degradation of reinforced concrete, f_{tres} = residual tensile strength, ε_{tres} = strain at which the residual tensile strength is attained.

Note 2: Two values are reported for M in each analysis, the first corresponding to the outermost vertical elements and the other to the interior vertical elements

Note 3: ε_0 = 0.002 and ε_u = 0.004 were assumed (for a reference length of 600mm) for the diagonal elements in all the simulations

Table 3 – Material Parameters for Reinforcing Steel

Specimen		f_y (MPa)	E_s (MPa)	β_h
Priestley et. al R1A	V	324	200000	0.046
	H	358		0.020
Priestley et. al R3A	V	467		0.020
	H	322		
Elwood & Moehle	V	479		0.020
	H	718		0.000

Note: f_y = yield stress, E_s = elastic modulus, β_h = ratio of hardening modulus over elastic modulus

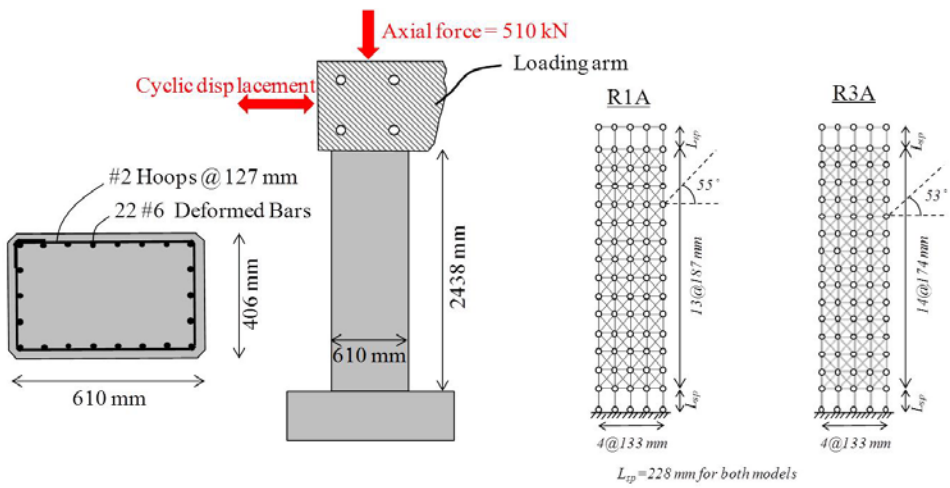

Fig. 6 – Test configuration for column specimens tested by Priestley et al. [26].

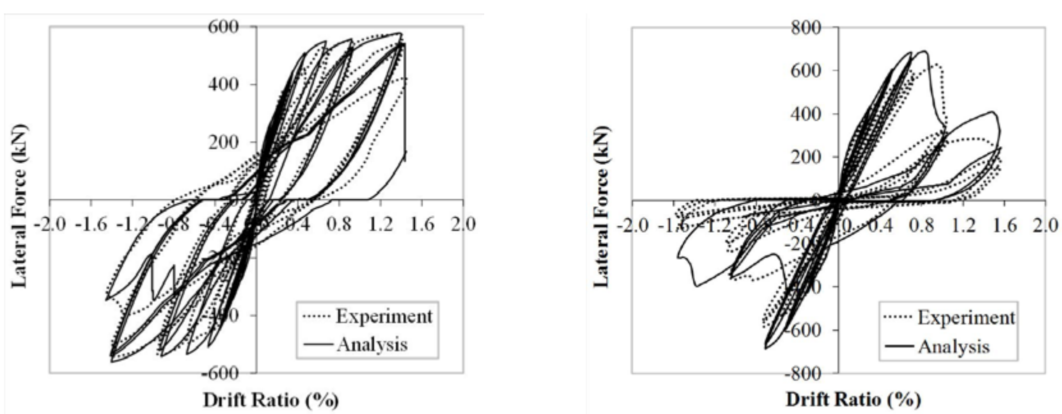

(a) Specimen R1A (b) Specimen R3A

Fig. 7 – Comparison of analytically obtained and experimentally recorded force-displacement response for column specimens tested by Priestley et al. [25].

To demonstrate the significance of accounting for the aggregate interlock effect in truss models of RC columns, the analysis for the R3A specimen tested by Priestley et al. [25] has been repeated, this time without including the contribution of the aggregate interlock in the shear resistance. The analysis gives the diagonal tension failure observed in the test, but it significantly underestimates the strength of the column, as shown in Fig. 9a, which compares the hysteretic response obtained for the analysis of column R3A without aggregate interlock to the experimentally obtained load-displacement curve.

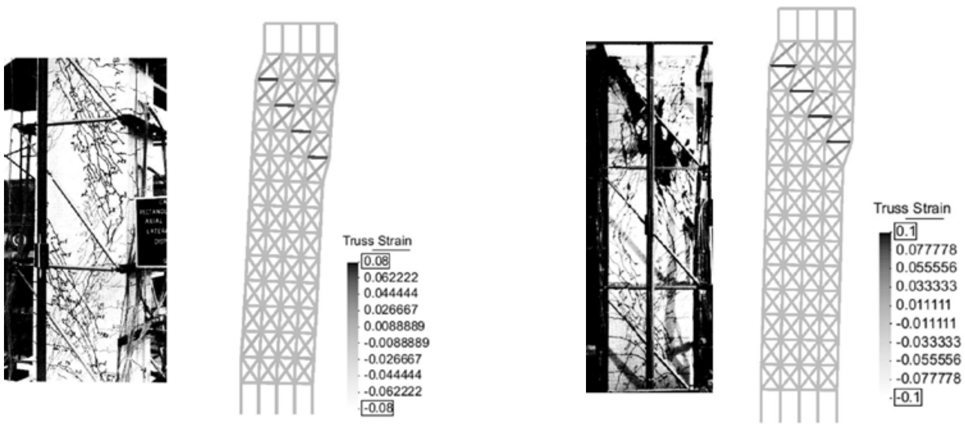

(a) Specimen R1A (b) Specimen R3A

Fig. 8 – Comparison of analytical and experimental damage patterns for column specimens tested by Priestley et al. [25] (deformations in analytical results magnified by a factor of 5).

Additionally, the effect of the inclination angle of the diagonal elements has been investigated for column R3A. More specifically, the analysis of the column, which had been conducted for $\theta_d = 53^o$, has been repeated for $\theta_d = 47^o$ and $\theta_d = 59^o$. The hysteretic curves obtained from the three analyses are compared in Fig. 9b. The analysis for $\theta_d = 47^o$ gives the same damage pattern as that shown in Fig. 8b. On the other hand, the analysis for $\theta_d = 59^o$ gives a flexure-dominated response, and no strength degradation due to shear damage is obtained. The significant increase of the cross-sectional area of the horizontal concrete and steel truss elements does not allow the occurrence of strength degradation associated with inclined diagonal cracking.

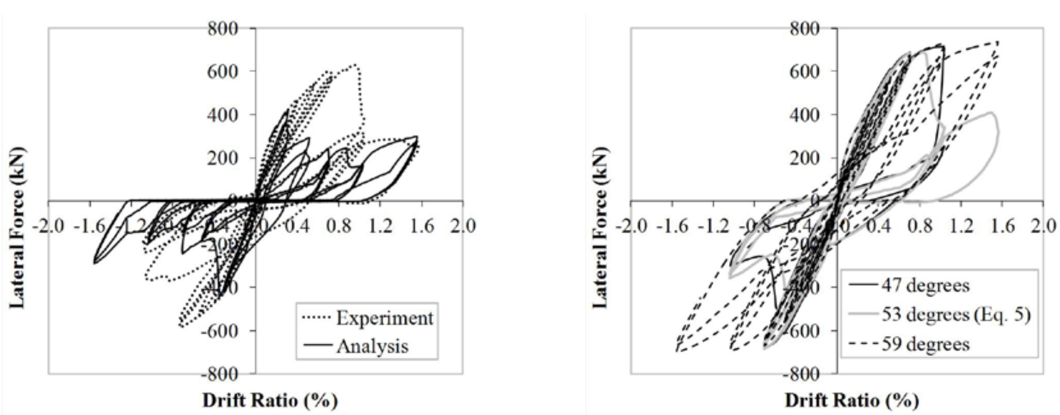

(a) Results without aggregate interlock effect (b) effect of angle, θ_d, of diagonal elements

Fig. 9 – Sensitivity study for column R3A tested by Priestley et al. [25].

3.2. Dynamic shake-table test

The proposed analysis method is also validated for dynamic loading using the results of the shake-table tests by Elwood and Moehle [26] on a half-scale, single-story, two-bay frame specimen. The concrete compressive and tensile strength were equal to 24.5 MPa (3.6 ksi) and 2.45 MPa (0.36 ksi), respectively, while the yield stress of the longitudinal steel reinforcement was equal to 479 MPa (69.7 ksi). To satisfy the scaling requirements, steel wires were used as transverse reinforcement. The yield stress of the wire reinforcement was equal to 718 MPa (104.5 ksi). The longitudinal reinforcement ratio was equal to 0.0252, while the transverse reinforcement ratio was equal to 0.0018. The specimen was subjected to a scaled version of a ground motion record from the 1985 Chile earthquake. The seismic excitation led to severe shear damage in the middle column.

The configuration of the specimen and of the corresponding analytical model is shown in Fig. 10. A truss assemblage is used for the middle column, while the other frame members are modeled by nonlinear beam elements having a fiber section. To account for the confinement effect, the compressive strength and ductility of the material in the core concrete fibers are increased using the equations by Mander et al. [27]. Rigid-end offsets are included in the connections of the beam elements. A Rayleigh viscous damping matrix, based on the initial stiffness matrix, is used in the analysis. A damping ratio of 2% is prescribed for the first and second modes of the system. Finally, a leaning column is added in the analytical model, to capture the effect of geometric nonlinearities resulting from the relatively large drift levels reached during the tests.

The analytically obtained hysteretic response and drift time histories are compared to their experimentally recorded counterparts in Figs. 11a and 11b. The major discrepancy is observed for the positive drift values, which are underestimated by the analysis after the occurrence of severe shear damage. The strength of the column is also overestimated by 19%. Still, the analytically obtained results can be considered as very satisfactory. The strength degradation in the analysis was associated with shear damage in the middle column, similarly to the damage pattern observed in the experimental test, as shown in Figs. 12a and 12b.

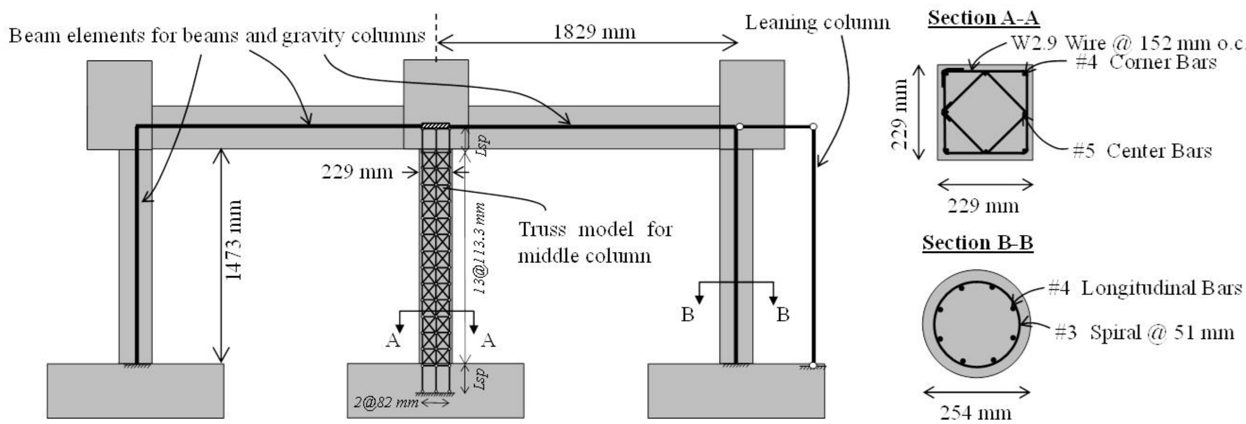

Fig. 10 – Configuration and analytical model for the shake-table specimen tested by Elwood and Moehle [26].

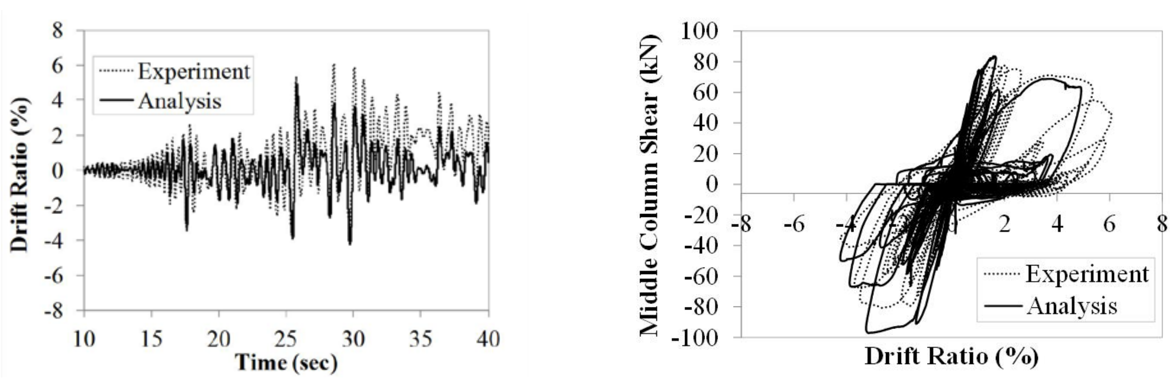

(a) Drift time history (b) Hysteretic response

Fig. 11 – Comparison of analytical and experimental results for the shake-table specimen tested by Elwood and Moehle [26].

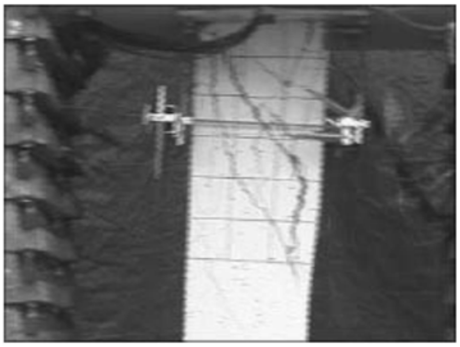

(a) Specimen damage at time t = 24.9s

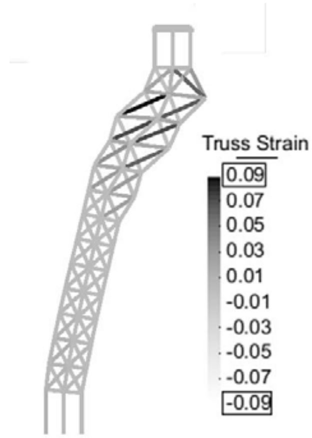

(b) Deformation (magnified by a factor of 5) at peak positive displacement in analysis (time t = 25.8s)

Fig. 12 – Comparison of analytical and experimental results for the shake-table specimen tested by Elwood and Moehle [26].

4. Conclusions

The truss analogy for reinforced concrete (RC) has been used to capture the nonlinear response of shear-critical RC columns. Existing constitutive models for concrete and reinforcing steel have been enhanced to capture the effect of aggregate interlock. A simple equation has been proposed for the determination of the inclination angle of the diagonal members in a truss model. The analysis approach was validated using data from quasi-static and dynamic experimental tests on shear-critical RC columns. The results obtained with the proposed methodology were in very good agreement with the experimental observations. Additionally, the importance of accounting for the aggregate interlock effect has been analytically demonstrated. The conceptual simplicity of the proposed methodology renders it suitable for the systematic analytical performance assessment of non-ductile RC construction in earthquake-prone areas.

5. References

[1] French S, Olshansky R (2001): Inventory of essential facilities in Mid-America, *Project SE-1 Final Report*, Mid-America Earthquake Center, University of Illinois at Urbana-Champaign, Urbana, IL.

[2] Beres A, White RN, Gergely P (1992): Seismic Behavior of Reinforced Concrete Frame Structures With Nonductile Details: Part I — Summary of Experimental Findings of Full Scale Beam-column Joint Tests, *Technical Report NCEER-92-0024*, National Center for Earthquake Engineering Research, State University of New York at Buffalo, Buffalo, NY.

[3] Hoffmann GW, Kunnath SK, Reinhorn AM, Mander JB (1992): Gravity-load-designed reinforced concrete buildings: Seismic evaluation of existing construction and detailing strategies for improved seismic resistance, *Technical Report NCEER-92-0016*, National Center for Earthquake Engineering Research, State University of New York at Buffalo, Buffalo, NY.

[4] ACI (2011): *Building Code Requirements for Structural Concrete, ACI 318-11*, American Concrete Institute.

[5] Elwood KJ (2004): Modelling failures in existing reinforced concrete columns, *Canadian Journal of Civil Engineering*, **31** (5), 846–859.

[6] Elwood K, Moehle J (2008): Dynamic Collapse Analysis For a Reinforced Concrete Frame Sustaining Shear and Axial Failures, *Earthquake Engineering and Structural Dynamics*, **37** (7), 991-1012.

[7] Leborgne MR, Ghannoum W (2013): Analytical Element for Simulating Lateral-Strength Degradation in Reinforced Concrete Columns and Other Frame Members, *ASCE Journal of Structural Engineering*, **140** (7), 04014038.

[8] Elwood K, Moehle J (2005a): Drift Capacity of Reinforced Concrete Columns with Light Transverse Reinforcement, *Earthquake Spectra*, **21** (1), 71-89.

[9] Leborgne MR (2012): Modeling the Post Shear Failure Behavior of Reinforced Concrete Columns, *Ph.D. Dissertation*, University of Texas, Austin, TX.

[10] Elwood K, Moehle J (2005b): Axial Capacity Model for Shear-Damaged Columns, *ACI Structural Journal*, **102** (4), 578-587.

[11] Li Y-J, and Ozbolt J (2002): Three-Dimensional Cyclic Analysis of Compressive Diagonal Shear Failure, *ACI Special Publication SP-205*, 61-80.

[12] Koutromanos I, Shing PB (2012): Cohesive crack model to simulate cyclic response of concrete and masonry structures," *ACI Structural Journal*, **109** (3), 349-358.

[13] Mazars J, Kotronis P, Davenne L (2002): A New Modeling Strategy for the Behavior of Shear Walls Under Dynamic Loading, *Earthquake Engineering and Structural Dynamics*, **31** (4), 937-954.

[14] Park H, Eom T (2007): Truss Model for Nonlinear Analysis of RC Members Subject to Cyclic Loading, *ASCE Journal of Structural Engineering*, **133** (10), 1351-1363.

[15] Panagiotou M, Restrepo J, Shoettler M, Kim G (2012): Nonlinear Cyclic Truss Model for Reinforced Concrete Walls, *ACI Structural Journal*, **109** (2), 205-214.

[16] Miki T, Niwa J (2004): Nonlinear Analysis of RC Structural Members Using 3D Lattice Model, *Journal of Advanced Concrete Technology*, **2** (3), 343-358.

[17] Lu Y, Panagiotou M (2013): Three-Dimensional Cyclic Beam-Truss Model for Non-Planar Reinforced Concrete Walls, *ASCE Journal of Structural Engineering*, **140** (3), 04013071.

[18] Moharrami M, Koutromanos I, Panagiotou M, Girgin SC (2015): Analysis of shear-dominated RC columns using the nonlinear truss analogy, *Earthquake Engineering & Structural Dynamics*, **44** (5), 677-694.

[19] Vecchio F, Collins M (1986): The Modified Compression-Field Theory for Reinforced Concrete Elements Subjected to Shear, *ACI Journal Proceedings*, **83** (2), 219-231.

[20] Bazant Z, Planas J (1998): *Fracture Processes in Concrete and Other Quasi-brittle Materials*, CRC Press, Boca Ratton, FL.

[21] Filippou F, Popov E, Bertero V (1983): Effects of Bond Deterioration on Hysteretic Behavior of Reinforced Concrete Joints, *Technical Report No. UCB/EERC-83/19*, Berkeley, CA.

[22] Walraven JC (1980): Aggregate Interlock: a Theoretical and Experimental Analysis, *PhD Dissertation*, TU Delft.

[23] Zhao J, Sritharan S (2007): Modeling of Strain Penetration Effects in Fiber-Based Analysis of Reinforced Concrete Structures, *ACI Structural Journal*, **104** (2), 133-141.

[24] McKenna F, Fenves GL, Scott MH, Jeremic B (2000): *Open System for Earthquake Engineering Simulation*.

[25] Priestley MJN, Seible F, Xiao Y, Verma R (1994): Steel Jacket Retrofitting of Reinforced Concrete Bridge Columns for Enhanced Shear Strength-Part 2: Test Results and Comparison with Theory, *ACI Structural Journal*, **91** (5), 537–551.

[26] Elwood K, Moehle J (2003): Shake Table Tests and Analytical Studies on the Gravity Load Collapse of Reinforced Concrete Frames, *Technical Report PEER 2003/01*, Pacific Earthquake Engineering Research Center, Berkeley, CA.

[27] Mander JB, Priestley MJN, Park R (1988): Theoretical stress-strain model for confined concrete, *ASCE Journal of Structural Engineering*, **114** (8), 1804–1826.